

A study on the use of the basement of the CEG building as bomb shelter

by
Luc de Wild

Dr. ir. P.C.J. Hoogenboom, Supervisor
Prof. Dr. H.M. Jonkers, Supervisor

Delft University of Technology
Delft, Zuid-Holland
June 25, 2024

Preface

This research is written for students of Civil Engineering with an interest in structural dynamics. Prior knowledge of structural mechanics, dynamics and numerical mathematics is recommended. Firstly, I would like to thank my supervisor Pierre Hoogenboom for helping me during the research and keeping me on track. Secondly, I would like to thank Henk Jonkers, for supervising me during the research. Lastly, I would like to thank the Technical management of the TU Delft for supplying the blueprints of the CEG building.

Summary

Due to the war in Ukraine, the threat of war with Russia has increased significantly. This thread has led to the question if the basement of the CEG faculty building can be used as a bomb shelter.

Before the basement of the CEG building can be used as a bomb shelter, practical requirements need to be met. Mainly, facilities as water and toilets need to be present to ensure a certain comfort when in use. Also, plans for the fastest route to the basement need to be present throughout the building in addition to the evacuation plans.

The ground floor of the building acts as the ceiling for the basement, this structural element will be tested for its resistance against explosive munitions. It is a reinforced concrete plate, with reinforcement bars orientated in two directions. To limit complexity, these orientations are considered separately.

The explosion of a munition produces a shock-wave that induces a load onto the reinforced concrete plate. The force exerted by this shock-wave is determined using an empirical graph and the Friedlander equation. Different explosive munitions employed by Russia are identified and the explosive properties determined.

The reinforced concrete plate can be modelled as a single-degree-of-freedom mass-spring system, for which an Ordinary differential equation is set up. The stiffness of the system is determined by analyzing the structural properties of the reinforced concrete plate. The plastic moment capacity is determined for 3 different locations, at which the beam is likely to break due to excessive loading. The plastic moment capacity of these points leads to the deflection and the corresponding load, from which the stiffness is determined. The beam undergoes three different stages of failure, for each stage a stiffness is determined. In combination with the load due to the shock wave, the ordinary differential equation can be solved. This is done with the Runge-Kutta method.

Results for the different explosive munitions show that the model is not sensitive for load due to a shock-wave, this is because of the high inertia of the system and the characteristic that the load is only applied for a very short amount of time. It is concluded that a mass-spring system is not suited model, when a reinforced concrete

plate is tested for explosive loads. Further research is needed which incorporates more locally orientated models.

Contents

Preface	i
Summary	ii
1 Introduction	1
1.1 Research	1
1.2 Research question	2
1.3 Structure	2
2 Practical use as bomb shelter	4
2.1 Exits	4
2.2 Basic facilities	4
2.3 Current use of the basement	5
3 Structural properties	6
3.1 Materials	6
3.2 Floor	6
4 Determining impact forces	9
4.1 Explosive pressure	9
4.2 Impact pressure	10
4.3 Explosive projectiles	11
4.3.1 OF-462 High Explosive Artillery shell	12
4.3.2 OF-45 High Explosive Artillery shell	12
4.3.3 OF-43 High Explosive Artillery shell	12
4.3.4 FAB-500 M62 High explosive aerial bomb	12
4.3.5 Iranian drones	12
5 Defining the mass-spring model	14
5.1 Equations for Single Mass Spring	14
5.2 Solving the ordinary differential equation	15
5.3 Reinforced concrete plate as a mass-spring system	15
5.4 Failure mechanism in the RC beam	16
5.4.1 Forming of plastic hinges in RC beam	17
5.4.2 Moment capacity in a cross section	18
5.4.3 Calculation of the deflections and the failure loads	20
5.5 Stiffness k of the system	22
5.6 Natural frequency	24

6 Solving the system	25
6.1 Initial conditions	25
6.2 Applied load due to shock-wave	25
6.3 Results	26
7 Discussion	29
7.1 Results	29
7.2 Mass-spring system	29
7.3 Reinforced concrete plate	29
7.4 Blast load	29
8 Conclusion	31
8.1 Answering research question	31
8.2 future research	31
A Model in python	33
B CEG blue print	39
C Forget-Me-Nots	40

Chapter 1

Introduction

For the past two years, Ukraine has been under attack by Russia, which seeks to expand its zone of influence. Since the collapse of the Soviet Union, a major conflict on the European continent was deemed very unlikely, but the western world was proven wrong. NATO and Europe feel the threat of the Russian aggression and military leadership urges countries and people to take this threat seriously¹. Although an attack against NATO and in particular The Netherlands would be still very unlikely, precautions are always valuable.

In conventional armed conflicts, the main battle is fought on the front line, but also behind the front line attacks are frequent. These attacks are mainly carried out by rockets, artillery shells and drones. Hiding in buildings is often not sufficient, because these suffer major damage and offer little protection when hit. The addition of bomb shelters would thus be very beneficial in certain densely populated areas behind the front line.

The campus of the TU Delft is such a place, where many people study and work daily. In the event of fighting on or near Dutch soil with an accompanying threat of attacks behind the front line, the presence of bomb shelters will be very valuable. This very much so the case for the TU Delft campus. A possible location for a bomb shelter in case of a threat is the basement of the faculty building of Civil Engineering and Geosciences (CEG). The faculty has a large basement, where many people could possibly take shelter when a threat is present. This possibility will be explored further in this report.

1.1 Research

This report will explore the possibility for the use of the CEG building as a bomb shelter. By analyzing the structure of the CEG building, in particular the basement, practical, spatial and structural properties are obtained.

Practical and spatial properties will determine the current state and use of the basement. On the basis of this information, alterations and additions for the practical use

¹Telegraaf online: ‘Dit zijn tekenen van groot Russisch offensief’, 22 maart 2024, Interview met oud-commandant der Landstrijdkrachten, Mart de Kruif, online: <https://www.telegraaf.nl/video/566840997/dit-zijn-tekenen-van-groot-russisch-offensief>

as a bomb shelter will be explored.

Another aim is to determine the impact resistance of the CEG building, in particular the structure of ground floor. The resistance to the impact of explosive munitions is a decisive factor in determining the possibility for the use of a bomb shelter.

This research focuses solely on the impact of a shock-wave produced by an explosive munition. The impact of an explosive munition may however contribute to other excessive loads placed on the structure of the ground floor. Parallel research is done by Feras Saab, focused on determining the loads placed on the floor plate due to the collapse of certain parts of the building (Saab, 2023).

1.2 Research question

The research can be summarized into the following research question.

Can the basement of CEG be used as a bomb shelter in wartime?

This question can be subdivided into multiple more confined questions to manage the scope of the research, while presenting it in a well-ordered way. These sub questions are listed below.

- What are the spatial properties of the CEG basement?
- What facilities must be present in a bomb shelter?
- What explosives are used, and how much load can they transfer onto the ground floor structure?
- How is the basement of CEG constructed, and what are the load-bearing elements?
- How can the ground floor structure be modelled as a mass-spring system?
- How can this model determine the failure load of the construction?
- Can the CEG basement resist the blast load of explosive munitions?

1.3 Structure

Chapter 2 delves into the practical considerations and requirements for the use as a bomb shelter, covering accessibility, exits and essential supplies. Chapter 3 examines the structural properties of the reinforced concrete plate. This includes an analysis of the used materials and design features. Chapter 4 focuses on the impact forces a bomb shelter faces, including blast wave propagation and the calculation of pressure on shelter surfaces. Frequently used explosive munitions are also listed and described. Chapter 5 introduces the mass-spring model as a theoretical approach to simulate the behavior of a reinforced concrete plate under impact forces. On the basis of structural mechanics, the strength of the construction is calculated. Subsequently, the Parameter values for the mass and stiffness of the model can be determined. Chapter

6 presents the numerical Runge-Kutta method for solving the ordinary differential equation of the mass-spring system equations of the mass-spring model. Different impacts are modelled and tests are done to determine the dynamic response of the model. Chapter 7 Evaluates the results, describing the dynamic response and presenting possible explanations. Finally, Chapter 8 draws conclusions, highlighting the main findings and their significance. It presents recommendations for future research and potential improvements in the model.

Chapter 2

Practical use as bomb shelter

Before a certain location can be used as a bomb shelter, different properties need to be known and requirements need to be met. This is to ensure the safety when in use.

2.1 Exits

Multiple exits are a requirement for shelters, due to unforeseen circumstances exits can get blocked. Changes for one exit to be blocked are low, but for multiple exits to be blocked, the changes are nearly negligible. More exits thus correspond to a safer bomb shelter.

The basement of the CEG faculty has an elongated shape, just as the building. The basement can be entered and left via multiple stairways and different other exits, such as a bicycle ramp. In the case of failure of the structure due to a blast load, it is likely this failure will be locally and will not affect the rest of the basement. It is thus very likely that there is an exit that can be used.

In the CEG building escape plans are already present, also in the basement escape plans are placed. In case the basement may be used as a bomb shelter, alternate plans need to be made and placed within the building. These plans display the protocol for an imminent threat and graphically give instructions on how to reach the basement safely.

2.2 Basic facilities

In the basement of the CEG faculty there are no toilets present. When the shelter is in use for a longer period of time, toilets are essential to ensure a certain comfort and dignity. A possible solution for this is to set up portable toilets when a threat is present.

Basic medical equipment is also needed in bomb shelters, in case of an accident or injury, it must be possible to perform basic medical procedures. These procedures can be performed by trained BHV personnel, of which multiple people are mandatory

to be present in a building.

The basement is ventilated by vent on both ends of the shelter. This might not be enough when many people take shelter. In the basement however, large ventilation devices are placed, which supply part of the building with air. When needed, these can be used for supplying the basement with air.

Water is a basic necessity in bomb shelters. When for any reason people are present for a longer period, water is essential for survival. Furthermore, it serves as a psychological comfort, in emergency situations access to water can help maintain a sense of control. In addition to water, the presence of other items such as blankets can comfort people taking shelter. When there is a possibility that shelter must be used, these facilities need to be present.

2.3 Current use of the basement

Currently much of the basement is used for storage. This includes several large objects as research equipment, and large trash bins. To ensure as much people can find shelter in the basement, these large objects must be moved. This means strategically relocating these object to other places in the basement.

Another part of the basement is used as a locked bicycle parking area, which takes up a significant part of the basement. During times of high threat, it is wise to close this area to bicycles, subsequently opening up more space for people. Moreover, the entrance to the bicycle area is accessible via a large open air ramp, this poses a dangerous situation if people take shelter in the basement. Explosive munitions might hit near this ramp, possibly causing a direct explosion in the basement. For use as a bomb shelter, this opening must be sealed off from the open air, to ensure the safety of the basement area.

Chapter 3

Structural properties

The CEG building was designed and constructed in the 1960s. Building materials and methods used at that period differ current from standards. To properly represent the strength of the construction elements in the model, the construction standards and material properties need to be known. On the basis of the blueprints of the CEG building shown in appendix B, these properties are determined.

3.1 Materials

Material properties have a large impact on the strength of a structural element. In the construction of the CEG building concrete class K-300 was used, in today's standards this would be class C19/22. This means that the characteristic strength for a concrete cylinder (f_{ck}) after 28 days of hardening is 19 N/mm^2 . With the current technology concrete classes go up to C100/110. The concrete used in the CEG building is thus not very strong in today's standards.

The steel used for reinforcement in 1968 was also less strong then it is nowadays. The reinforcement steel used has a yield stress (f_{yk}) of 410 MPa. Compared to the 500 MPa as the current standard, it varies less than the concrete but still forms a significant difference.

To ensure that imperfections in these materials do not lead to premature failure, safety factors are included in the model. For concrete a safety factor of $\gamma_c = 1.5$ is applied, this leads to the following compressive strength, $f_{cd} = f_{ck}/\gamma_c = 19/1.5 = 12.6 \text{ N/mm}^2$. Steel has a safety factor of $\gamma_s = 1.15$, this leads to a tensile strength of $f_{yd} = f_{yk}/\gamma_s = 410/1.15 = 356.5 \text{ N/mm}^2$.

3.2 Floor

Along the CEG building, the Ground floor is mostly constructed as a reinforced concrete plate, that is cast in situ. The blueprint of this floor construction between section 53 and 63 is shown in figure 3.1 and appendix B. The reinforcement of the floor runs in two perpendicular directions, subsequently forming a reinforcement net. However, the steel bars can only counteract loading forces, in one primary directions. Because of this, the floor must be tested in these two primary directions, in which the reinforcement is orientated.

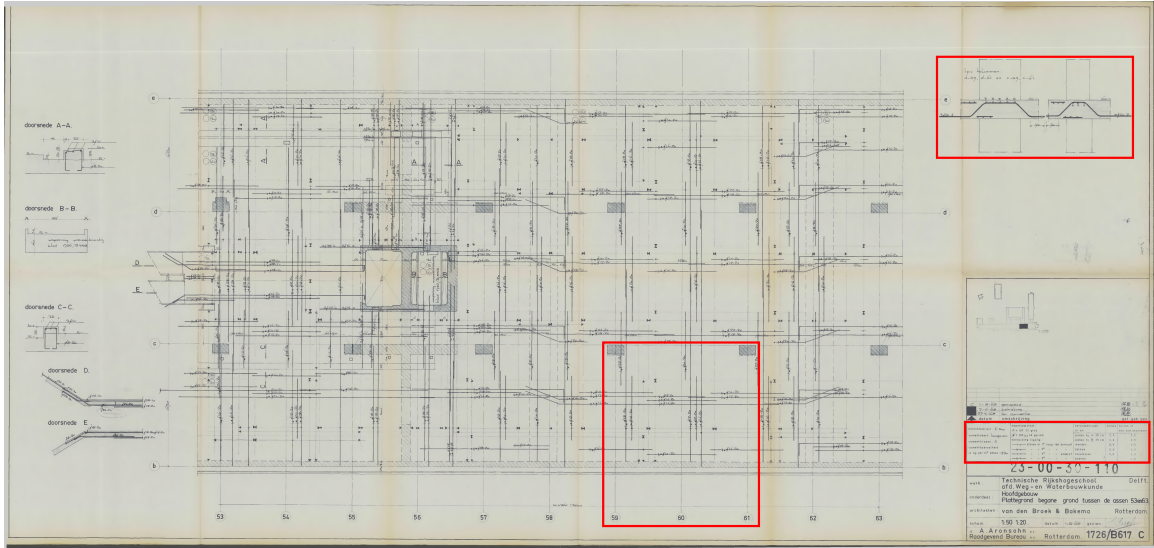


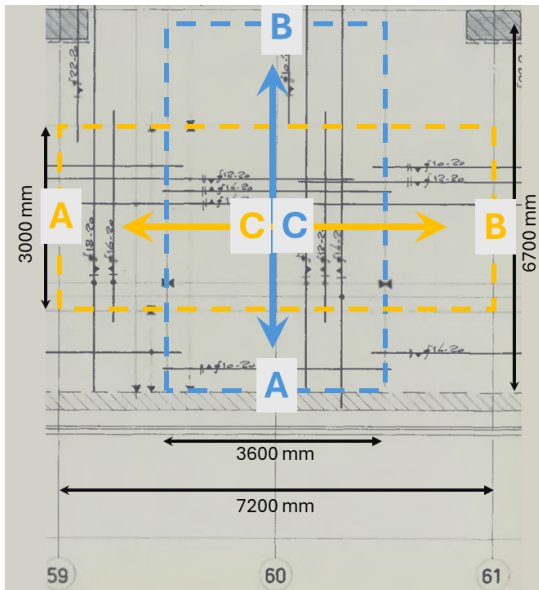
Figure 3.1: blueprint of floor construction between section 53 and 63, details of figure 3.2 in red. (Aronsohn, A. (Van den Broek & Bakema), 1968)

The structural properties of the floor can be determined using the blueprint. Figures 3.2(a) and 3.2(b) display the details for the floor properties between sections 59 and 61 of the CEG building. In figure 3.2(c), the notation used in the blueprints is shown. These can be explained as follows: $\phi 12 - 20$ means that there are reinforcement bars present with a diameter of 12 millimeters and a center line spacing of 20 centimeters (5 reinforcement bars per meter). The triangles facing upwards or downwards (\blacktriangle \blacktriangledown) mean that the reinforcement is placed at the top and bottom of the cross-section respectively. Left of these triangles, one or two lines define if the reinforcement is placed in the first or second layer from the outside (see figure 3.2c). The placement in the first or second layer has influence on the over of the reinforcement bars, see section ???. Figure 3.2a shows the reinforcement directions that are tested in the model. The yellow section follows the reinforcement bars placed parallel to the building, the blue section follows the reinforcement bars placed perpendicular to the building.

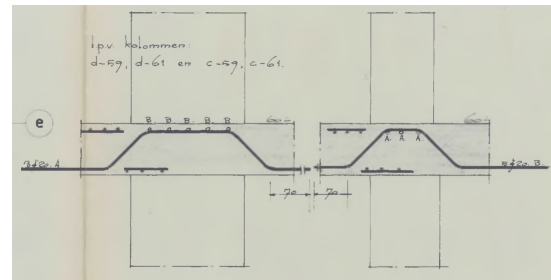
For the modelling of the reinforced concrete plate, the properties of the plate and reinforcement steel are listed in table 3.1. The properties are determined at approximately the middle of this rectangular section. In the middle of the plate, the reinforcement at the bottom of the cross-section is modelled. At the ends of the plate, the reinforcement at the top of the cross-section is modelled. This is done, because these reinforcement bars are loaded in tension, see section 5.4.

Table 3.1: Properties of reinforced concrete plate used in the model

	Reinforcement Parallel to building	Reinforcement Perpendicular to building
Span (<i>mm</i>)	7200	6700
Width (<i>mm</i>)	3000	3600
Height (<i>mm</i>)	600	600
$A_{s,A}$ (mm^2)	$15 \times 10 + 15 \times 12$	18×12
$A_{s,B}$ (mm^2)	$15 \times 10 + 15 \times 12$	$18 \times 12 + 18 \times 10$
$A_{s,C}$ (mm^2)	30×14	$18 \times 12 + 18 \times 14$
Cover A,B (<i>mm</i>)	20 + 18	20
Cover C (<i>mm</i>)	20 + 14	20



(a) Floor plate blue print



(b) Details column and floor plate

betonkwaliteit: K 20	wapeningsstaal $\phi = OR\ 24$ glad	betondekkingen in cm	betondekkingen	
			binnen	buiten of niet controleerbaar
cementsaort: Δ	$\phi = OR(p)$ 42 geribd	platen $h_t < 20$ cm	1,0	2,5
cementklasse: Δ	oanduiding ligging	platen $h_t \geq 20$ cm	2,0	3,5
in kg per m ³ beton: 330	— staven in 1 ^e laag van bovenaf	wanden	2,0	3,5
	— — — 2 ^e — — —	balken	2,0	3,5
	— — — 1 ^e — — — onderaf	kolommen	3,0	4,0
	— — — 2 ^e — — —	poeren	—	4,0

(c) Notation used in the blue prints

Figure 3.2: Details of floor plate between sections 59 and 61 (Aronsohn, A. (Van den Broek & Bakema), 1968)

Chapter 4

Determining impact forces

When a bomb explodes, a chemical reaction creates an exothermic reaction, which creates gasses that rapidly expand, subsequently forming a shock wave. This type of load is called air shock. So-called high explosive munitions use a shock wave as primary effect to cause damage to a target. To determine what damage an explosive can do to the CEG building, the properties and energy transfer of the shock wave need to be determined.

4.1 Explosive pressure

Explosives are the propelling power behind shock waves. It is therefore important that these explosives can be quantified, this is usually done in TNT-equivalent weight. Using equation 4.1 the TNT-equivalent weight of an explosive munition can be calculated (Weggel, 2010).

$W_{P_{TNT}}$ is the TNT-equivalent weight in kg, P is the relative explosive power of the substance compared to TNT. W is the weight in kg of the explosive substance. P_{TNT} is the explosive power of TNT, and is equal to 1.0. The TNT-equivalent weight of different munitions is calculated in section 4.3.

$$W_{P_{TNT}} = \left(\frac{P}{P_{TNT}} \right) W \quad (4.1)$$

The explosion can take place at a certain distance with respect to the beam. The further away the explosion takes place, the lower the impact force of the shock wave will be. The 'cube-root' scaling law can be applied to account for this distance from the explosion to the beam, Weggel (2010). Z is the scaled distance, R is the distance from the explosion to the midpoint of the structure, in this case the center of the beam. W is the TNT-equivalent weight of the explosive substance in the munition. The scaled distances of different munitions and locations are calculated in 4.3

$$Z = R/W^{1/3} \quad (4.2)$$

4.2 Impact pressure

Shock waves travelling through air produce a force when encountering an object. Figure 4.1 can be used to determine the parameters necessary for the calculation of the shock wave force. Using the scaled distance Z from equation 4.2, the time it takes for the shock wave to reach the object is parameter t_a . The pressure at this instant is P_r , this pressure increase happens in only a few nanoseconds and is thus not included. The third relevant parameter is the positive pressure phase duration of the shock wave (t_0). The data in the figure is empirically determined, this means that for every scaled distance Z , the parameter values need to be read. The reading of the figure must be precise, because small reading errors can have large parameter differences due to the two logarithmic scales.

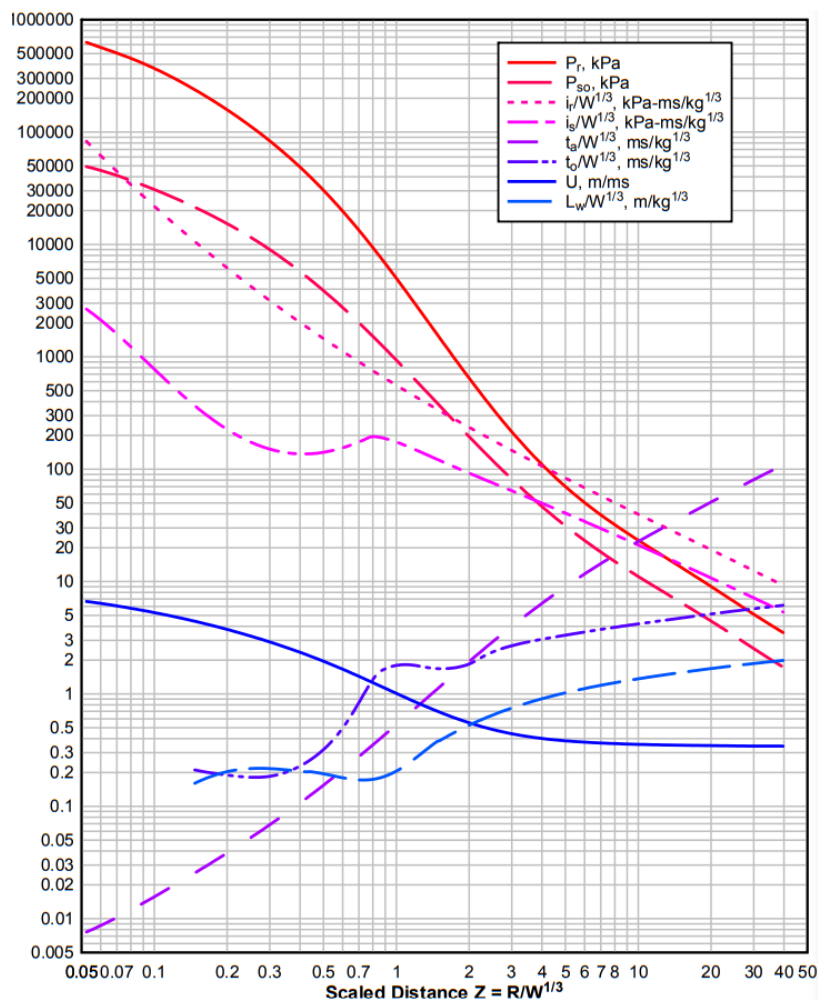


Figure 4.1: Positive Phase Shock Wave Parameters for a Spherical TNT Explosion in Free Air at Sea Level, Engineers of U.S. Army Corps (2008)

To determine what force is applied to the reinforced concrete plate, the previously mentioned parameters can be applied to the Friedlander equation (4.3). This equation

calculates the force applied by the shockwave as a function of time. The Friedlander equation is a proven accurate approach of the pressure produced by an explosive shock wave. By implementing small increments of Δt , the function is essentially integrated, leading to the impulse produced by the shock wave (equation 4.4). The duration of the positive pressure phase produced by the shock wave is t_0 , a graphical representation of the pressure is given in figure 4.2.

$$P_s(t) = P_r \left(1 - \left(\frac{t - t_a}{t_0} \right) \right) e^{-\left(\frac{t - t_a}{t_0} \right)} \quad (4.3)$$

$$I_s = \int_{t_a}^{t_a+t_0} P_r \left(1 - \left(\frac{t - t_a}{t_0} \right) \right) e^{-(t-t_a)} dt \quad (4.4)$$

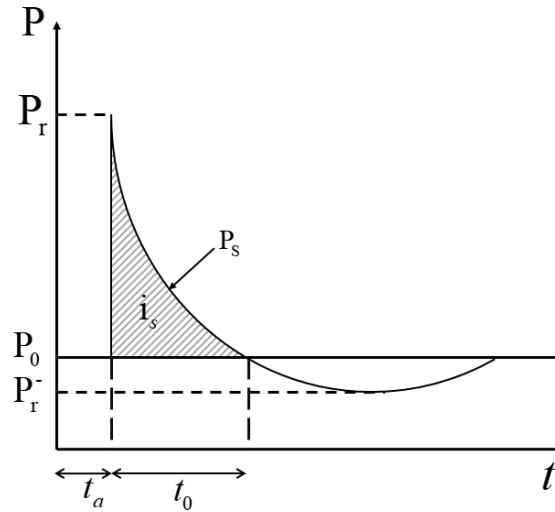


Figure 4.2: Blast pressure pulse (Karlos V. and Solomos G., 2013)

The explosion of a munition is usually triggered by hitting something. In this case that is the facade of the CEG building. The impact of the munition be at different heights with respect to the reinforced concrete floor plate of the ground floor. Furthermore, the explosion has a different impact on the two reinforcement directions. This is shown in figure 4.3a where the munition hits the facade, and figure 4.3b where the perspective is rotated 90 degrees. The distributed load is not equal across the length of the plate in both directions. To accommodate for this, the distributed load is simplified to be uniform across the plate (figure 4.3c), the magnitude will be determined in section 5.3. This description of the load is only valid for this particular scenario.

4.3 Explosive projectiles

Different types of munitions are currently used by Russia in Ukraine. To determine to what extent the basement of CEG can be used as a bomb shelter, these different

munitions need to be identified. Furthermore, the properties of the munitions need to be known, in particular the explosive power.

This shell also expels fragmentation of the casing, however little information is available of this. Determining the size and speed of these particles is difficult with little information. In addition, it is likely that many fragments end up in the facade.

4.3.1 OF-462 High Explosive Artillery shell

The OF-462 is the smallest Artillery shell that will be tested. It has an explosive load of 3460 grams of TNT and a diameter of 122 mm. (GICHHD, 2022)

4.3.2 OF-45 High Explosive Artillery shell

A frequently used projectile in Ukraine is the Russian made OF-45 High Explosive Artillery shell. This shell has a diameter of 152 mm and is loaded with 7650 grams of A-IX-2, which is an explosive substance made in Russia (GICHHD, 2022). It has a TNT-equivalent explosive power of 1.54 (GICHHD, 2017).

4.3.3 OF-43 High Explosive Artillery shell

Another artillery shell that is used in Russia is the OF-43 high explosive artillery shell. It has a diameter of 203 mm and is loaded with 17800 grams of A-IX-2 (GICHHD, 2022). This shell has a lot more explosive power than the OF-45.

4.3.4 FAB-500 M62 High explosive aerial bomb

The FAB-500 M62 is a less accurate munition. However, it is heavily loaded, with 209000 gram of TNT (GICHHD, 2022). When the munitions mentioned above do not lead to failure of the structure, this aerial bomb will be tested to look for the limits of the structure.

4.3.5 Iranian drones

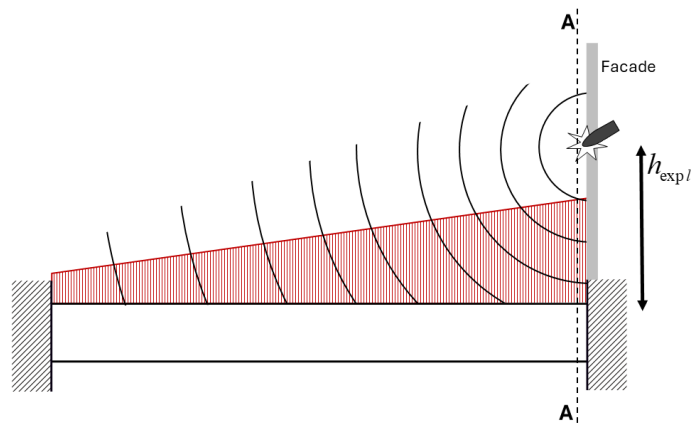
Another way Russia targets Ukrainian targets is with the use of unmanned drones. The Shahed models 136 and 136 are commonly used. These drones are manufactured in Iran and have a relatively low cost. The Shahed 131 model has an explosive warhead of approximately 10 to 15 kilograms (no information on the substance) and a range of 900 kilometers (World Today News, 2023). These drones can thus be used to attack targets far behind the front line. The 136 model is approximately twice as big and can carry an explosive load of about 40 kilograms (RFE/RL, 2024).

Example OF-45 using equation 4.1:

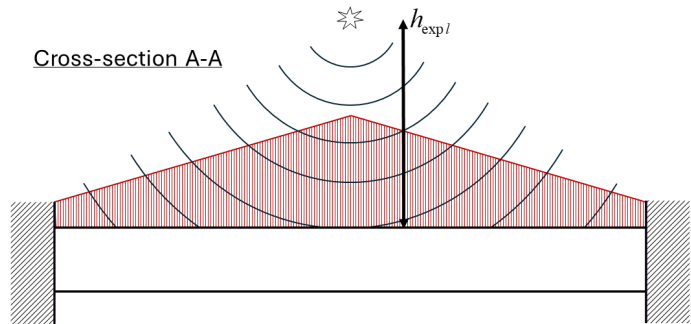
$$W_{P_{TNT}} = \left(\frac{P}{P_{TNT}} \right) W = \left(\frac{1.54}{1.00} \right) 7.65 = 11.78kg$$

Table 4.1: Explosive properties of explosive munitions

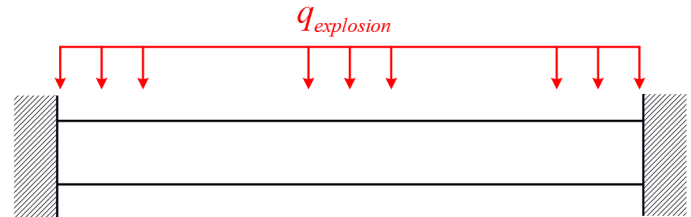
	Explosive substance	Weight (kg) W	Relative explosive power P	TNT-equivalent weigh (kg) $W_{P_{TNT}}$	
	OF-465	TNT	3.46	1.00	3.46
	OF-45	A-IX-2	7.65	1.54	11.78
	OF-43	A-IX-2	17.80	1.54	27.41
	Shahed 131	TNT	15.00	1.00	15.00
	Shahed 136	TNT	40	1.00	40.00
	FAB-500	TNT	209.00	1.00	209.00



(a) Explosion from side perspective



(b) Explosion from cross-section A-A perspective



(c) Resulting distributed load due to explosion

Figure 4.3: Shock wave and subsequent loading onto a fixed plate

Chapter 5

Defining the mass-spring model

To analyze the impact on the basement structure and subsequently determining the reaction, a model is needed. This model will be a simplification of a reinforced concrete plate, represented by a single mass spring system.

5.1 Equations for Single Mass Spring

The reinforced concrete plate can be modelled as a mass spring system with a single degree of freedom, this is visualized in figure 5.1. The equation of motion (eq. 5.1) describes the behavior of the system as a function of time t in terms of acceleration \ddot{w} , velocity \dot{w} and deflection from the zero position w . The parameters m is the mass, c is the damping coefficient which subtracts energy from the system and k is the stiffness of the spring. Energy is added to the system by the function $f(t)$ which is a force that is applied as a function of time t .

$$m\ddot{w} + c\dot{w} + kw = f(t) \quad \text{with} \quad \begin{cases} \dot{w}(t) = v(t) \\ \ddot{w}(t) = \dot{v}(t) = a(t) \end{cases} \quad (5.1)$$

The damping coefficient c is neglected in the model, because this coefficient has little effect on the deflection, when an RC beam is subjected to an explosive load (Baker et al., 1983).

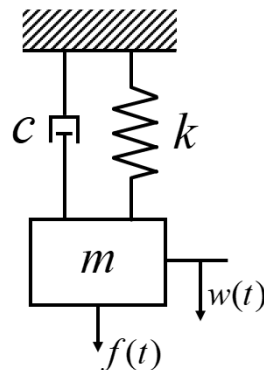


Figure 5.1: Mass-spring-damper system

5.2 Solving the ordinary differential equation

The equation of mass spring system is an ordinary differential equation (ODE), which can be solved using numerical methods. The method used for solving this ODE is the Runge-Kutta (RK4) method. This method is a higher order method, which has attractive stability properties and results in large savings (Vuik et al., 2016). However, for the RK4 method, four small increments are calculated for every time step, which increases the computational power needed. For the scope of this model however, this forms an arbitrary increase in computational time.

Equation 5.1 can be written in matrix and vector form, as shown in equation 5.2a, with simplification for 5.2b for mathematical operations and $\vec{y} = \begin{pmatrix} \dot{w} \\ w \end{pmatrix}$

$$\begin{bmatrix} m & 0 \\ 0 & 1 \end{bmatrix} \begin{pmatrix} \ddot{w} \\ \dot{w} \end{pmatrix} + \begin{bmatrix} c & k \\ -1 & 0 \end{bmatrix} \begin{pmatrix} \dot{w} \\ w \end{pmatrix} = \begin{pmatrix} f(t) \\ 0 \end{pmatrix} \quad (5.2a)$$

$$[A]\vec{y} + [B]\vec{y} = \vec{F} \quad (5.2b)$$

The RK4 method approximates the solution at the next time step with by

$$\vec{y}_{t+1} = \vec{y}_t + \frac{1}{6}(k_1 + 2k_2 + 2k_3 + k_4) \quad (5.3)$$

k_1 to k_4 are estimators and are given by

$$\begin{aligned} k_1 &= \Delta t \vec{G}(\vec{y}_t, t) \\ k_2 &= \Delta t \vec{G}(\vec{y}_t + \frac{1}{2}k_1, t + \frac{1}{2}\Delta t) \\ k_3 &= \Delta t \vec{G}(\vec{y}_t + \frac{1}{2}k_2, t + \frac{1}{2}\Delta t) \\ k_4 &= \Delta t \vec{G}(\vec{y}_t + k_3, t + \Delta t) \end{aligned} \quad (5.4)$$

$\vec{G}(\vec{y}_t, t)$ is the function, acquired from the Euler forward method, as shown in equation 5.5

$$\vec{y} = [A]^{-1} \cdot (\vec{F} - [B]\vec{y}_t) = \vec{G}(\vec{y}, t) \quad (5.5)$$

5.3 Reinforced concrete plate as a mass-spring system

To represent the plate as a single degree of freedom system, adjustments and simplifications need to be made. The plate has two directions in which the reinforcement is placed. These directions will separately be modelled as a reinforced concrete beam, to limit the complexity of the model. Based on the boundary conditions, different factors are used. Firstly, the load-factor: the beam is loaded with a distributed load

q due to a shock wave. Not all load transferred onto the beam is represented in the system, this is done by applying a load-factor. Secondly the mass-factor: In the representation as a single-mass-spring system, not all mass of the beam will be present, the mass-factor accounts for this (Engineers of U.S. Army Corps, 2008). The load and mass factors can be combined into a single factor, the Load-Mass factor (K_{LM}). Furthermore, these factors differ for the elastic and plastic stage of the deformation. To account for this, a factor for a combined 'elasto-plastic' deformation is present. Because the deformation of the RC beam includes both the elastic and plastic regions, this factor will be used within the model. The different factors are displayed in table 5.1. The implementation of the Load-Mass factor in the ODE is displayed in equation 5.6.

$$K_{LM} \cdot m\ddot{w} + c_v\dot{w} + kw = f(t) \quad (5.6)$$

Table 5.1: Transformation factors for beam, fixed on both sides (Engineers of U.S. Army Corps, 2008)

Range Behavior	Load factor k_L	Mass factor k_M	Load-Mass factor k_M
<i>Elastic</i>	0.53	0.41	0.77
<i>Elasto-plastic</i>	0.64	0.50	0.78
<i>Plastic</i>	0.50	0.33	0.66

5.4 Failure mechanism in the RC beam

When a fixed supported beam is loaded by a distributed load, the moment distribution shown in figure 5.2 is present in the beam. Due to the load, the material will deflect and produce a counteracting force. When the applied force is bigger than the maximum counteracting force the beam can produce, the beam fails. The counteracting force produced by the beam is the result of the materials and properties of the beam. A failing beam means that the material has reached it maximum strength, after which it yields and a plastic hinge forms. For the total failure of a fixed supported beam, three plastic hinges need to form. The locations at which these hinges form is wherever in the beam the bending moment exceeds the moment capacity at that location.

Before plastic hinges form the beam deflects, equation 5.7 describes this deflection for a fixed supported beam (see figure 5.5 situation 1)

$$w_C = \frac{1}{384} \frac{q_0 L^4}{EI_C} \quad (5.7)$$

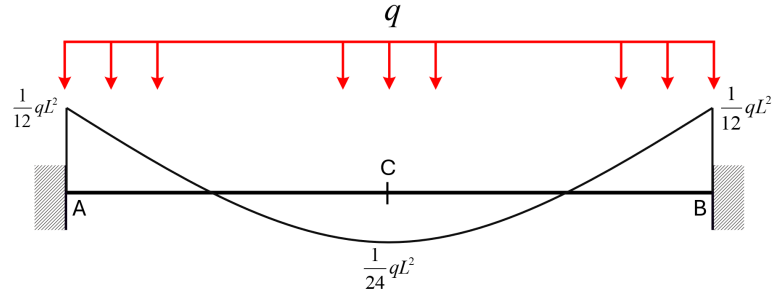


Figure 5.2: Moment distribution for a beam fixed at both ends.

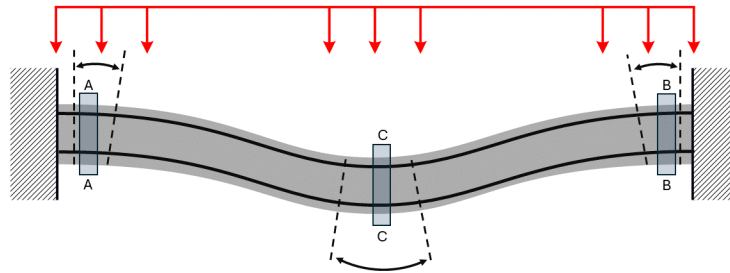


Figure 5.3: Deflection of a fixed reinforced concrete beam before failure

5.4.1 Forming of plastic hinges in RC beam

At cross-sections A and B the bending moment due to the distributed load is the highest. At these points, the first plastic hinges form.

When cross-sections A and B have different structural properties, the moment capacities also differ. As a consequence, the cross-section with the lowest moment capacity will fail first. For the perpendicular reinforcement, cross-section A has less steel and thus a lower moment capacity (see table 3.1)

At a certain distributed load, the cross-section at A reaches its moment capacity and a plastic hinge S_A forms. When a plastic hinge forms, this point cannot resist a load increase and undergoes plastic deformation as is shown in figure 5.5, situation 2.

After the failure of point A, further increasing the load increases the bending moment at cross-section B. Subsequently a hinge at point B begins to form, this is shown in situation 3. When cross-section A and B have the structural properties, hinges A and B form simultaneously.

For a total failure of the RC beam to occur, three plastic hinges need to form. The third plastic hinge forms at cross-section C, after which a failure mechanism leads to the total failure of the beam (situation 5).

5.4.2 Moment capacity in a cross section

At a fixed supported beam three plastic hinges form at cross-sections A, B and C. The reinforcement steel in tension in the cross-section is primarily responsible for the moment capacity of a beam. In Cross-sections A, B and C, the reinforcement steel in tension is located differently, this is shown in figure 5.4.

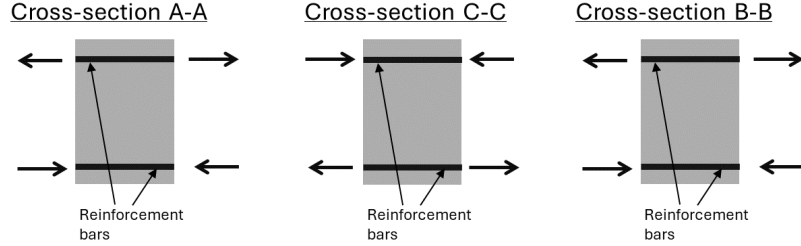


Figure 5.4: Tensile and compressive forces in Cross-sections A, B and C

The moment capacity of a cross-section can be calculated with equations 5.8a and 5.8b (Braam and Lagendijk, 2011).

$$M = A_s \cdot f_{yd} \cdot (d - \beta \cdot x_u) \quad (5.8a)$$

$$x_u = \frac{A_s \cdot f_{yd}}{\alpha \cdot b \cdot f_{cd}} \quad (5.8b)$$

with:

A_s	$[mm^2]$	Surface area of the reinforcement steel in tension.
d	$[mm]$	Depth of the reinforcement steel
b	$[mm]$	Width of the cross-section
f_{yd}	$[N/mm^2]$	Design yield strength of the reinforcement steel (= 356.5)
f_{cd}	$[N/mm^2]$	Design compressive strength of the concrete (= 12.6)
α	$[-]$	Constant (= 0.75)
β	$[-]$	Constant (= $\frac{7}{18}$)

To determine the stiffness EI of the reinforced concrete beam, the curvature of the beam at the maximum moment capacity can be calculated by

$$\kappa = \frac{\varepsilon_c}{x_u} \quad (5.9)$$

With ε_c being the compression of the concrete at the maximum moment capacity (= 3.5‰). Finally, the stiffness EI of the beam can be determined with

$$EI = \frac{M_{pl}}{\kappa} \quad (5.10)$$

Given these equations and the properties at this cross-section, the moment capacity can be calculated. First the surface area of the reinforcement steel can be calculated (15 with diameter 10 and 15 bars with diameter 12).

$$A_{s,A} = \frac{1}{4}\pi \cdot D^2 \cdot bars = \frac{1}{4}\pi \cdot 10^2 \cdot 15 + \frac{1}{4}\pi \cdot 12^2 \cdot 15 = 2875 \text{ mm}^2$$

The depth of the reinforcement concrete is calculated with the height of the cross-section (600 mm), the concrete cover and the diameter reinforcement bars.

$$d = h - cover - \frac{1}{2} \cdot D_{s,A} = 600 - 38 - \frac{1}{2} \cdot 12 = 556 \text{ mm}$$

Given a width of 3000 mm, equations 5.8a and 5.8b can be filled in and calculated.

$$x_u = \frac{A_s \cdot f_{yd}}{\alpha \cdot b \cdot f_{cd}} = \frac{2875 \cdot 356.5}{0.75 \cdot 3000 \cdot 12.6} = 36.2 \text{ mm}$$

$$M_{pl} = A_s \cdot f_{yd} \cdot (d - \beta \cdot x_u) = 2875 \cdot 356.5 \cdot \left(556 - \frac{7}{18} \cdot 36.2\right) = 5.55 \cdot 10^8 \text{ Nmm}$$

$$\kappa = \frac{\varepsilon_c}{x_u} = \frac{3.5 \cdot 10^{-3}}{36.2} = 9.68 \cdot 10^{-5} \text{ m}^{-1}$$

$$EI = \frac{M_{pl}}{\kappa} = \frac{5.55 \cdot 10^8}{9.68 \cdot 10^{-5}} = 5.74 \cdot 10^{12} \text{ Nmm}^2$$

These calculations are also done for the other cross-sections, the values are listed in table 5.2

Table 5.2: Parameters and calculated values of the moment capacity for every cross-section

Cross-section	Parallel Reinforcement			Perpendicular Reinforcement		
	A	B	C	A	B	C
A_s [mm^2]	2875	2875	3393	2035	3449	4806
d [m]	556	556	560	573	573	573
x_u [m]	36.2	36.2	42.7	21.3	36.2	50.4
b [m]	3000	3000	3000	3600	3600	3600
M_{pl} [Nmm]	$5.55 \cdot 10^8$	$5.55 \cdot 10^8$	$6.57 \cdot 10^8$	$4.01 \cdot 10^8$	$6.88 \cdot 10^8$	$9.49 \cdot 10^8$
κ [m^{-1}]	$9.68 \cdot 10^{-5}$	$9.68 \cdot 10^{-5}$	$8.20 \cdot 10^{-5}$	$16.40 \cdot 10^{-5}$	$9.68 \cdot 10^{-5}$	$6.95 \cdot 10^{-5}$
EI [Nmm^2]	$5.74 \cdot 10^{12}$	$5.74 \cdot 10^{12}$	$8.02 \cdot 10^{12}$	$2.50 \cdot 10^{12}$	$7.10 \cdot 10^{12}$	$13.65 \cdot 10^{12}$

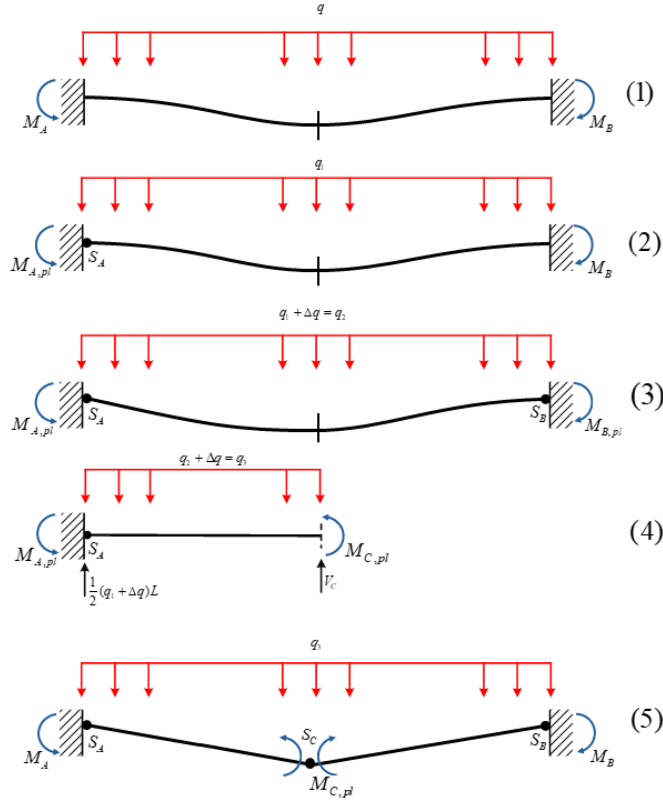


Figure 5.5: Failure mechanism for fixed beam

5.4.3 Calculation of the deflections and the failure loads

Assuming that the properties of cross-sections A and B are not identical, plastic hinges A and B form separately. At first, a plastic hinge forms at point A (figure 5.5, situation 2). Using the boundary condition that the slope of the beam at both fixed points is zero ($\theta_A = 0$), the needed distributed load can be determined. Using the 'forget-me-nots' 7 and 9 from appendix C, equation 5.11 with $M_B = M_{A,pl}$ can be solved, giving: $q_1 = \frac{12M_{A,pl}}{L^2}$. The deflection at the midpoint C can be calculated with equation 5.12 which is based also on 'forget-me-nots' 4 and 6.

$$\theta_A = \frac{1}{48} \frac{q_1 L^3}{EI_C} - \frac{1}{4} \frac{M_{A,pl} L}{EI_C} = 0 \quad (5.11)$$

$$w_{C,1} = \frac{1}{192} \frac{q_1 L^4}{EI_C} - \frac{1}{32} \frac{M_{A,pl} L^2}{EI_C} \quad (5.12)$$

For cross-section A of the perpendicular reinforcement, the following values can be calculated:

$$q_1 = \frac{12M_{A,pl}}{L^2} = \frac{12 \cdot 4.01 \cdot 10^8}{6700^2} = 108 \text{ N/mm}$$

$$w_{C,1} = \frac{1}{192} \frac{q_1 L^4}{EI_C} - \frac{1}{32} \frac{M_{A,pl} L^2}{EI_C} = \frac{1}{192} \frac{108 \cdot 6700^4}{13.65 \cdot 10^{12}} - \frac{1}{32} \frac{4.01 \cdot 10^8 \cdot 6700^2}{13.65 \cdot 10^{12}} = 42.1 \text{ mm}$$

Equation 5.11 and 5.12 are based on the 'forget-me-nots', however these standard formulas assume a beam with a uniform EI , which is not the case in the RC beam. To accommodate for this, the slope and deflection are based on the forces and EI from that particular section of the beam. This should give a reasonable approach for the slope and deflection of the beam at these points, but an error is present in the calculations, which should be taken into account.

The forming of the second hinge (figure 5.5, situation 3) can be calculated by the condition that $\theta_B = 0$. Given this condition and using 'forget-me-nots' 4 and 6, equation 5.13 is formed. By solving this equation for q_2 the following value is found $q_2 = 8 \frac{M_{B,pl}}{L^2} + 4 \frac{M_{A,pl}}{L^2}$. The deflection can now be determined by using the same 'forget-me-nots' and is shown in equation 5.14

$$\theta_B = \frac{1}{24} \frac{q_2 L^3}{EI_C} - \frac{1}{3} \frac{M_{B,pl} L}{EI_C} - \frac{1}{6} \frac{M_{A,pl} L}{EI_C} = 0 \quad (5.13)$$

$$w_c = \frac{5}{384} \frac{q_2 L^4}{EI_C} - \frac{1}{16} \frac{M_{A,pl} L^2}{EI_C} - \frac{1}{16} \frac{M_{B,pl} L^2}{EI_C} \quad (5.14)$$

Equations 5.13 and 5.14 are also based on the same assumptions as the previous equations. An error is thus present, which must be taken into account.

For cross-section B of the perpendicular reinforcement, the following values can be calculated:

$$\begin{aligned} q_2 &= 8 \frac{M_{B,pl}}{L^2} + 4 \frac{M_{A,pl}}{L^2} = 8 \frac{6.88 \cdot 10^8}{6700^2} + 4 \frac{4.10 \cdot 10^8}{6700^2} = 159 \text{ N/mm} \\ w_c &= \frac{5}{384} \frac{q_2 L^4}{EI_C} - \frac{1}{16} \frac{M_{A,pl} L^2}{EI_C} - \frac{1}{16} \frac{M_{B,pl} L^2}{EI_C} \\ &= \frac{5}{384} \frac{159 \cdot 6700^4}{13.65 \cdot 10^{12}} - \frac{1}{16} \frac{4.01 \cdot 10^8 \cdot 6700^2}{13.65 \cdot 10^{12}} - \frac{1}{16} \frac{6.88 \cdot 10^8 \cdot 6700^2}{13.65 \cdot 10^{12}} = 80.1 \text{ mm} \end{aligned}$$

For the total failure of the beam a third plastic hinge must form. It is assumed that this hinge forms at the middle of the beam, for which the distributed load can be calculated by solving equation 5.15. Implementing the distributed load into equation 5.16, the deflection at which the beam fails is obtained.

$$\sum T|_C = -M_{A,pl} - M_{C,pl} - q_3 \cdot \frac{L}{2} \cdot \frac{L}{4} - \left(\frac{1}{2} \cdot q_3 \cdot L \right) \cdot \frac{L}{2} = 0 \quad (5.15)$$

$$w_c = \frac{5}{384} \frac{q_3 L^4}{EI_C} - \frac{1}{16} \frac{M_{A,pl} L^2}{EI_C} - \frac{1}{16} \frac{M_{B,pl} L^2}{EI_C} \quad (5.16)$$

The values of q_3 and $w_{C,3}$ for the perpendicular reinforcement can now be calculated.

$$\begin{aligned} \sum T|_C &= -M_{A,pl} - M_{C,pl} - q_3 \cdot \frac{L}{2} \cdot \frac{L}{4} - \left(\frac{1}{2} \cdot q_3 \cdot L \right) \cdot \frac{L}{2} \\ &= -4.01 \cdot 10^8 - 9.49 \cdot 10^8 - q_3 \cdot \frac{6700}{2} \cdot \frac{6700}{4} - \left(\frac{1}{2} \cdot q_3 \cdot 6700 \right) \cdot \frac{6700}{2} = 0 \\ &\rightarrow q_3 = 242 \text{ N/mm} \end{aligned}$$

$$\begin{aligned} w_c &= \frac{5}{384} \frac{q_3 L^4}{EI_C} - \frac{1}{16} \frac{M_{A,pl} L^2}{EI_C} - \frac{1}{16} \frac{M_{B,pl} L^2}{EI_C} \\ &= \frac{5}{384} \frac{242 \cdot 6700^4}{13.65 \cdot 10^{12}} - \frac{1}{16} \frac{4.01 \cdot 10^8 \cdot 6700^2}{13.65 \cdot 10^{12}} - \frac{1}{16} \frac{6.88 \cdot 10^8 \cdot 6700^2}{13.65 \cdot 10^{12}} = 239.7 \text{ mm} \end{aligned}$$

Table 5.3: Distributed load and deflection at the forming of the hinges as cross-section A, B and C

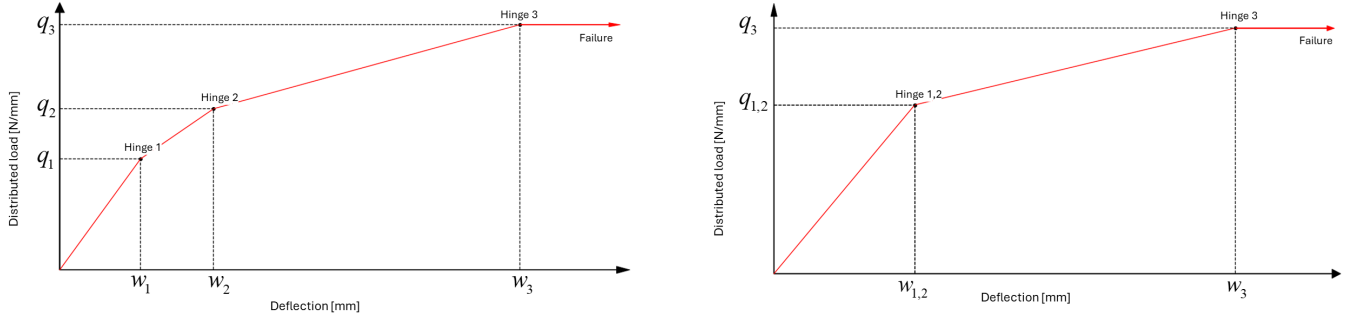
	Parallel reinforcement	Perpendicular reinforcement
q_1 [N/mm]	129	108
q_2 [N/mm]	129	159
q_3 [N/mm]	187	242
$w_{C,1}$ [mm]	112.3	40.2
$w_{C,2}$ [mm]	112.3	80.1
$w_{C,3}$ [mm]	368.0	239.7

5.5 Stiffness k of the system

The deflection and distributed load for fixed supported beam is graphically represented in figure 5.6.

Given the values of the deflection and the magnitude of the distributed load, the stiffness k can be calculated by taking the slope between the forming of the hinges. The distributed load is multiplied by the length of the beam to find the stiffness in N/mm .

$$k = \frac{(q_{i+1} - q_i)}{w_{C,i+1} - w_{C,i}} \quad (5.17)$$



(a) Deflection and distributed load form non-uniform cross-sections A and B (b) Deflection and distributed load form uniform cross-sections A and B

Figure 5.6: Forming of plastic hinges related to deflection and distributed load

After the formation of hinge 3, the slope is zero and the stiffness of the system is subsequently also zero. This means that the resistance of reinforced concrete against deformation is zero. For the perpendicular reinforcement, the following stiffnesses are found.

$$k_1 = \frac{(q_1 - q_0)L}{w_{C,1} - w_{C,0}} = \frac{(108 - 0) \cdot 6700}{42.1 - 0} = 17187 N/mm$$

$$k_2 = \frac{(159 - 108) \cdot 6700}{80.1 - 42.1} = 8992 N/mm, \quad k_3 = \frac{(242 - 159) \cdot 6700}{239.7 - 80.1} = 3484 N/mm$$

Table 5.4: Stiffness of the system between the forming of hinges, till

	Parallel reinforcement	Perpendicular reinforcement
k_1 [N/mm]	8271	17187
k_2 [N/mm]	8271	8992
k_3 [N/mm]	1633	3484
k_4 [N/mm]	0	0

The stiffness k of the system can now be written as

$$k = \begin{cases} k_1, & w < w_{C,1} \\ k_2, & w_{C,1} < w < w_{C,2} \\ k_3, & w_{C,2} < w < w_{C,3} \\ 0, & w > w_{C,3} \end{cases} \quad (5.18)$$

5.6 Natural frequency

With the mass and the stiffness in the unbroken state known, the natural frequency can be determined. using the following equation

$$f = \frac{\omega_0}{2\pi} \quad \text{with} \quad \omega_0 = \sqrt{\frac{k}{m}} \quad (5.19)$$

with w_0 in rad/s, k in N/m and m in kg. For the parallel orientated reinforced beam, this gives

$$m = b \cdot h \cdot L \cdot \rho_c = 3000 \cdot 600 \cdot 7200 \cdot 2650 \cdot 10^{-9} = 34344.0 \text{ kg}$$

$$w_0 = \sqrt{\frac{k}{m}} = \sqrt{\frac{8271 \cdot 10^3}{34344.0}} = 15.5 \text{ rad/s}$$

$$f = \frac{\omega_0}{2\pi} = \frac{15.5}{2\pi} = 2.47 \text{ Hz}$$

For the perpendicular orientated reinforced beam, this gives

$$m = b \cdot h \cdot L \cdot \rho_c = 3200 \cdot 600 \cdot 6700 \cdot 2650 \cdot 10^{-9} = 38350.8 \text{ kg}$$

$$w_0 = \sqrt{\frac{k}{m}} = \sqrt{\frac{17187 \cdot 10^3}{38350.8}} = 21.2 \text{ rad/s}$$

$$f = \frac{\omega_0}{2\pi} = \frac{21.2}{2\pi} = 3.37 \text{ Hz}$$

Chapter 6

Solving the system

6.1 Initial conditions

All the parameters of the mass-spring system are now known and the system can be solved. The starting position and velocity of the mass are determined first. The starting velocity of the mass is zero, the starting deflection of the mass can be determined for both the parallel and perpendicular reinforcement orientations using equation 5.7 and the mass of the beam per meter.

Parallel orientated Reinforcement

$$q_0 = b \cdot h \cdot \rho_c \cdot g = 3000 \cdot 6000 \cdot 2650 \cdot 9.81 \cdot 10^{-9} = 45.2N/mm$$

$$w_C = \frac{1}{384} \frac{q_0 L^4}{EI_C} = \frac{1}{384} \frac{45.2 \cdot 7200^4}{8.02 \cdot 10^{12}} = 39.4mm$$

Perpendicular orientated Reinforcement

$$q_0 = b \cdot h \cdot \rho_c \cdot g = 3200 \cdot 6000 \cdot 2650 \cdot 9.81 \cdot 10^{-9} = 49.9N/mm$$

$$w_C = \frac{1}{384} \frac{q_0 L^4}{EI_C} = \frac{1}{384} \frac{49.9 \cdot 6700^4}{13.65 \cdot 10^{12}} = 19.2mm$$

These deflections are not the same, however they do occur at the same point in the two-dimensional plane. This will be further discussed in the discussion of the results (see chapter 7).

6.2 Applied load due to shock-wave

The load applied to the system due to the shock-wave is dependent on the height of the explosion (see figure 4.1 and equation 4.2). The height of the explosion above the floor plate is 1 meter for the tests.

This gives the explosive munitions the following scaled distance to the center of the beam ($R = 1 m$)

Table 6.1: Calculated scaled distance, t_0 and P_{SO} for every munition at a height of 1 meter

	TNT-equivalent weigh [kg] $W_{P_{TNT}}$	scaled distance Z [m]	t_0 [$ms/kg^{1/3}$]	P_r [kPa]
OF-465	3.46	0.66	0.70	13000
OF-45	11.78	0.44	0.25	35000
OF-43	27.41	0.33	0.20	60000
Shahed 131	15.00	0.41	0.23	45000
Shahed 136	40.00	0.29	0.18	85000
FAB-500	209.00	0.17	0.19	200000

t_0 ranges from $0.70 \cdot 3.46 = 2.4$ and $0.19 \cdot 209 = 39.7$ milliseconds, which is important when modelling the blast. To properly model the blast for every t , the time step Δt must be small enough for the Friedlander equation to properly be applied (see equation 4.4). It is determined that this Δt must be 1/100th of a millisecond, or 0.00001 seconds.

6.3 Results

All munitions are tested in the model. Figures 6.1 to 6.6 show the deflection of the reinforced concrete plate, subjected to the explosive blasts of the munitions. The figures are divided in the parallel and the perpendicular orientations of the reinforce concrete plate.

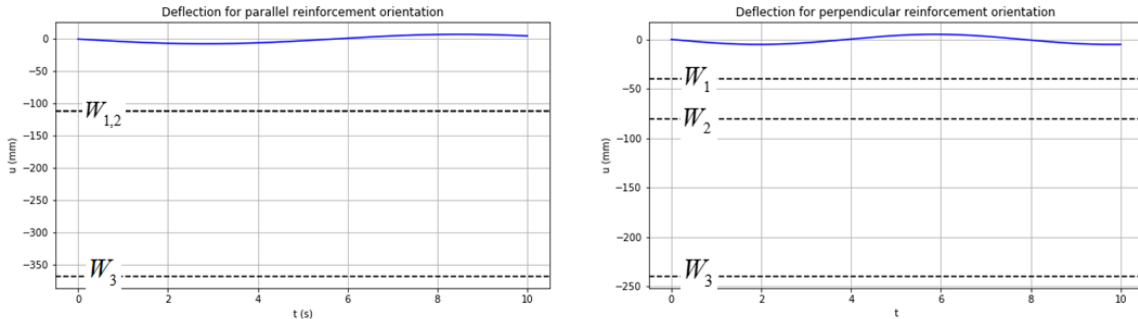


Figure 6.1: Dynamic response of the OF-465 HE artillery shell, $W_{P,TNT} = 3.46$ kg, $t_0 = 1.1$ ms, $P_r = 13000$ kPa

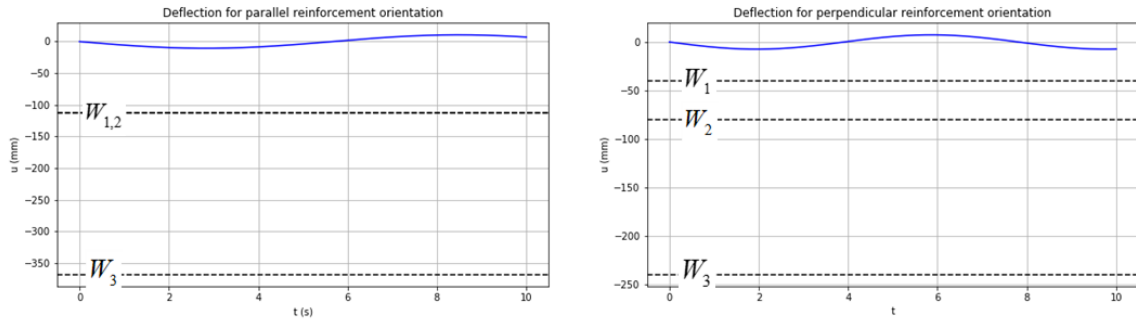


Figure 6.2: Dynamic response of the OF-45 HE artillery shell, $W_{P,TNT} = 11.78 \text{ kg}$, $t_0 = 0.5 \text{ ms}$, $P_r = 35000 \text{ kPa}$

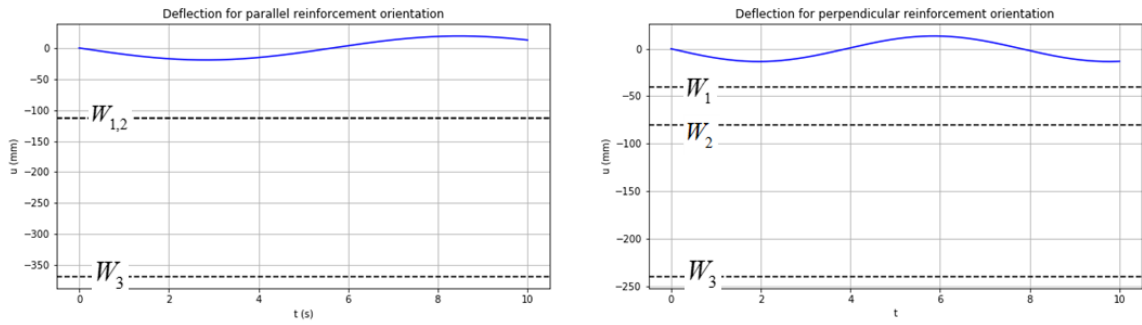


Figure 6.3: Dynamic response of the OF-43 HE artillery shell, $W_{P,TNT} = 27.41 \text{ kg}$, $t_0 = 0.6 \text{ ms}$, $P_r = 60000 \text{ kPa}$

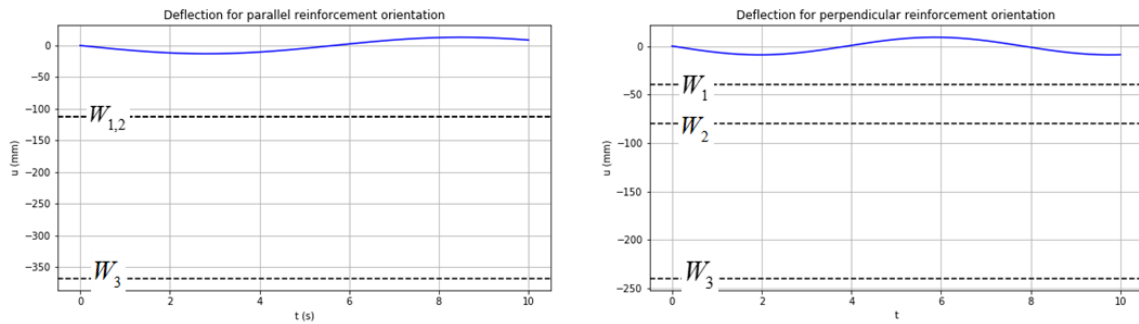


Figure 6.4: Dynamic response of the Shahed 131 drone, $W_{P,TNT} = 15.0 \text{ kg}$, $t_0 = 0.06 \text{ ms}$, $P_r = 45000 \text{ kPa}$

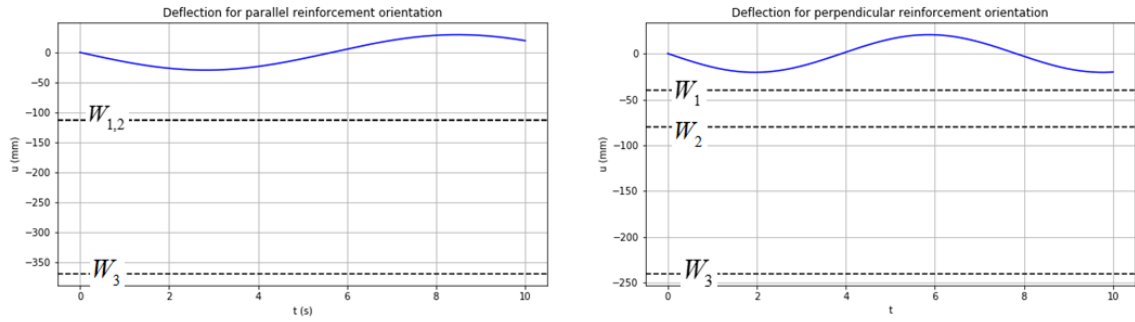


Figure 6.5: Dynamic response of the Shahed 136 drone, $W_{P,TNT} = 40.0 \text{ kg}$, $t_0 = 0.06 \text{ ms}$, $P_r = 85000 \text{ kPa}$

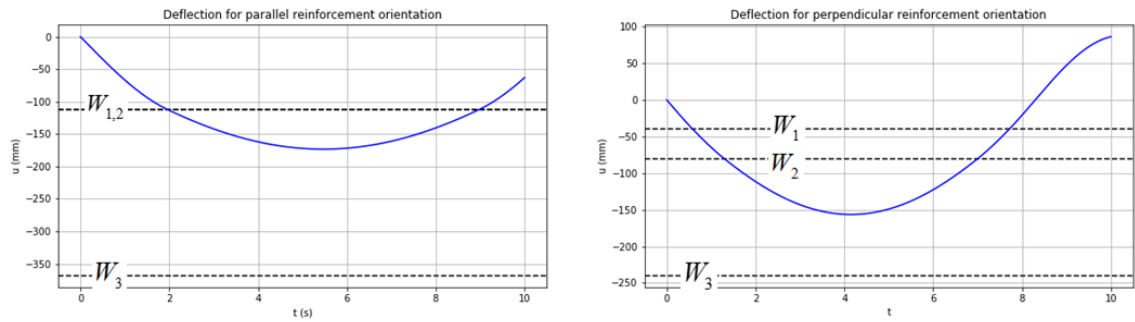


Figure 6.6: Dynamic response of the FAB-500 aerial bomb, $W_{P,TNT} = 209.0 \text{ kg}$, $t_0 = 1.1 \text{ ms}$, $P_r = 200000 \text{ kPa}$

Chapter 7

Discussion

7.1 Results

Figures 6.1 to 6.4 show that no plastic hinge form in the reinforced concrete plate. For these explosive munitions, the reinforced plate will thus not fail. However, for the explosive load produced by the FAB-500 aerial bomb, two plastic hinges form in both the parallel and perpendicular orientations of the reinforced concrete plate. Figure 6.6 shows that the mass of the system will move back to the null-position after two plastic hinges have formed, in reality this however will not happen, because the plastic deformation is permanent.

For the total failure and subsequent collapse of the reinforced concrete plate, a third hinge must form. In all situations, a third hinge does not form.

7.2 Mass-spring system

To determine if the reinforced concrete plate can withstand a blast from an explosive projectile, simplifications were made to make the problem more commutable and intuitive. Firstly, the deflection of the beam is represented as a single degree of freedom mass spring system, in which a part of the beam forms the mass and the bending stiffness forms the spring stiffness. This is a simplification to approximate the complex system, which consists of many more variables and conditions.

7.3 Reinforced concrete plate

The reinforced concrete plate is divided in two reinforcement orientations, which are both modelled as separate reinforced concrete beams. This however takes away the added structural benefits that this orientation has. Moreover, because of complexity, the corners of the reinforced concrete plate are not considered and modelled.

7.4 Blast load

The blast load that is modelled assumes that the load is instantaneously evenly spread on the plate. However, the main characteristic of a shock wave is that travels and the

pressure decreases as the moves away from its origin. The load will thus not spread evenly, furthermore the load will not arrive at every location on the plate at the same time, which may induce other dynamic responses.

The explosion, assumed in this research, originates from the facade of the building. Due to a shock wave, the middle of the beam is loaded, however in reality the blast can originate from an off center position as well.

The blast from the munition is initiated by hitting something, in this case the facade of the CEG building. Some of the explosive energy will also be transferred to the object that is hit by the munition. However, in the model it is assumed that the explosion takes place in an open space near the beam. The blast load will thus likely be greater than when actually hitting the facade of the CEG building.

Chapter 8

Conclusion

8.1 Answering research question

For the reinforced concrete plate of the ground floor of the CEG building, modeled as a mass-spring system and subjected to an evenly spread explosive load, the structure does not collapse for the tested explosive munitions.

For the basement to be able to be used as a bomb shelter, the current spatial layout and use must be altered to accommodate more people. Also basic facilities must be present in the basement, such as water, temporary toilets and medical equipment. The open air bicycle creates a dangerous situation, and must be shielded in some way.

8.2 future research

In the mass-spring system, the mass, stiffness and explosive loads are assumed to be global parameters. Further research can be done on local response in the reinforced concrete plate. An example of a locally orientated model is the finite element method. This method determines the stiffness, deflection and explosive load, for small sections across the plate and what influence they have on each other. This could give valuable insights in the dynamic response of the ground floor structure.

Part of the ground floor structure which covers the basement is not located between walls, so vehicles can pass under the CEG building. Explosive munitions can directly hit the ground floor structure. For the use as a bomb shelter, research can be done on a direct impact in this section.

Not much is known about how many people daily visit the CEG building and how many people are present at peak moments. More research is needed to determine if the basement is large enough to shelter all present in the building.

The Campus of the TU Delft is very large and many people visit each day. The basement of the CEG building cannot shelter all these people, moreover not every

one will be close enough to reach the basement. It would thus be valuable to study if other buildings and can be used as a bomb shelter.

Appendix A. Model in python

The python model makes use of two files. In the first file the functions used for calculating are defined, in second file the calculations take place and the model is tested.

Failure of a cross-section

```
In [1]: # Calculating the Moment capacity, the curvature, the beamstiffness and x_u
def func_4(cover, A_s):
    d = h - cover - 0.5*o_hw
    x_u = (A_s * f_yd) / (0.75 * b * f_cd)
    M4 = A_s * f_yd * (d - (7/18) * x_u)
    kappa4 = (3.5 * 1e-3) / (x_u)
    EI4 = M4 / kappa4
    return M4, kappa4, EI4, x_u
```

Deflection for every hinge formed

```
In [2]: # Calculating the deflection for 0 hinges
def func_w0():
    q0 = (2650 * b * h * 1e-9) * 9.81
    w_C0 = (1/384) * ((q0 * (L**4)) / (EI_C))
    return q0, w_C0

# Calculating the deflection for 1 hinge
def func_w1():
    q1 = (12 * M_pl_A) / (L**2)
    w_C1 = ((1/192) * ((q1 * (L**4)) / (EI_C)) - ((1/32) * ((M_pl_A * (L**2)) / (EI_C))
    return q1, w_C1

# Calculating the deflection for 2 hinges
def func_w2():
    q2 = 8 * (M_pl_B / (L**2)) + 4 * (M_pl_A / (L**2))
    w_C2 = ((5/384) * ((q2 * (L**4)) / (EI_C)) - ((1/16) * ((M_pl_A * (L**2)) / (EI_C)) - ((1/16) * ((M_pl_B * (L**2)) / (EI_C))
    return q2, w_C2

# calculating the deflection at which at third hinge forms
def func_w3():
    dq = symbols('dq')
    equation = + M_pl_A + M_pl_C + (dq) * (L/2) * (L/4) - ((1/2) * (dq) * L) * (L/2)
    delta_q = solve(equation)[0]
    q3 = delta_q
    w_C3 = ((5/384) * ((q3 * (L**4)) / (EI_C)) - ((1/16) * ((M_pl_A * (L**2)) / (EI_C)) - ((1/16) * ((M_pl_B * (L**2)) / (EI_C))
    return q3, w_C3
```

Stiffness

```
In [3]: # Defining the stiffness of the system for a distributed Load per mm
def func_k():
    k1 = (q1 * L) / w_C1
    k2 = ((q2 - q1) * L) / (w_C2 - w_C1)
    k3 = ((q3 - q2) * L) / (w_C3 - w_C2)
    k4 = 0
    return k1, k2, k3, k4

# function for changing the stiffness for increasing deflections
def func_stiffness(u):
    if u == 0:
        return k1
    elif u < -w_C3:
        return k4
    elif u < -w_C2:
        return k3
    elif u < -w_C1:
        return k2
    else:
        return k1
```

Explosion

```
In [4]: # Calculating the pressure and positive phase duration
def func_expl_par(W_TNT):
    P_R = P_r * 1e-3 # pressur fromm kPa to N/mm^2
    t_0 = t0 * (W_TNT**(1/3)) * 1e-3 # Positive phase duration
    return P_R, t_0

# Friedland equation
def func_friedland(t):
    pressure = P_R * (1 - (t / t_0)) * np.exp(-(t / t_0))
    return pressure # N/mm^2
```

Running ODE and RK4

```
In [5]: # Function for the shock wave in time
def func_ft(t):
    if t <= t_0:
        f_t = func_friedland(t) * b * L
    else:
        f_t = 0
    return np.array([-f_t, 0.0])

# Function for the RK4 method
def func_G(y, t, A_inv, B):
    G = np.dot(A_inv, (func_ft(t) - np.dot(B,y))) # setting up the equation
    return G

# Calculating the RK4 method
def func_RK4(y, t, dt, A_inv, B):
    k_1 = func_G(y, t, A_inv, B)
    k_2 = func_G(y + 0.5*k_1*dt, t + 0.5*dt, A_inv, B)
    k_3 = func_G(y + 0.5*k_2*dt, t + 0.5*dt, A_inv, B)
    k_4 = func_G(y + k_3 *dt, t + dt, A_inv, B)
    RK4 = (dt * (k_1 + 2*k_2 + 2*k_3 + k_4)) / 6
    return RK4

# Solving the equation with the RK4 method
def func_run(y0, timesteps, dt):
    A_inv = inv(np.array([[m * K_LM, 0], [0, 1]])) # inverse of matrix A
    y = y0
    w = []
    v = []
    f = []
    for t in timesteps:
        k = func_stiffness(y[1])
        B = np.array([[c, k], [-1, 0]]) # matrix B
        RK4 = func_RK4(y, t, dt, A_inv, B)
        y = y + RK4
        v.append(y[0])
        w.append(y[1])
        f.append(func_ft(t)[0])
        if y[1] < -w_C3 or t == timesteps[-1]:
            break
    return v, w, f
```

```
In [1]: import os
import numpy as np
import pandas as pd
from sympy import symbols, solve
from matplotlib import pyplot as plt
from scipy.integrate import odeint
from labellines import labelline, labellines
from numpy.linalg import inv
%run FunctionsBEP.ipynb
```

Plate parameters

```
In [2]: %run FunctionsBEP.ipynb
def func_parallel():
    L = 7200
    b = 3000
    h = 600
    cover_AB = 20 + 18
    cover_C = 20 + 14
    o_hw = 12
    A_s_A = ((1/4) * np.pi * (10**2) * 15) + ((1/4) * np.pi * (12**2) * 15)
    A_s_B = ((1/4) * np.pi * (10**2) * 15) + ((1/4) * np.pi * (12**2) * 15)
    A_s_C = ((1/4) * np.pi * (12**2) * 30)
    m = L * b * h * 2650 * 1e-9
    return L, b, h, cover_AB, cover_C, o_hw, A_s_A, A_s_B, A_s_C, m

def func_perpendicular():
    L = 6700
    b = 3600
    h = 600
    cover_AB = 20
    cover_C = 20
    o_hw = 14
    A_s_A = ((1/4) * np.pi * (12**2) * 18)
    A_s_B = ((1/4) * np.pi * (12**2) * 18) + ((1/4) * np.pi * (10**2) * 18)
    A_s_C = ((1/4) * np.pi * (12**2) * 18) + ((1/4) * np.pi * (14**2) * 18)
    m = L * b * h * 2650 * 1e-9
    return L, b, h, cover_AB, cover_C, o_hw, A_s_A, A_s_B, A_s_C, m

L, b, h, cover_AB, cover_C, o_hw, A_s_A, A_s_B, A_s_C, m = func_parallel()
L, b, h, cover_AB, cover_C, o_hw, A_s_A, A_s_B, A_s_C, m = func_perpendicular()
```

```
In [3]: %run FunctionsBEP.ipynb
f_yd = 356.6 # Steel yield strength (N/mm^2)
f_cd = 12.6 # Design value for compressive strength of concrete
E_s = (200 * 1e3) # Elastic modulus of steel (N/mm^2)
K_LM = 0.78 # Load-mass transformation factor
eps_c3 = (1.75 * 1e-3) # Limit value of concrete under compression (promile)

# Explosives
P_TNT = 1.00
W_OF_465 = 3.46
W_OF_45 = 11.78
W_OF_43 = 27.41
W_SH_131 = 15.0
W_SH_136 = 40.0
W_FAB_500 = 209
```

```
In [4]: %run FunctionsBEP.ipynb
# System properties as t=0
c_s = 0 # Dampingsconstante (N/m)
t_start = 0 # begintijd (s)
dt = 0.00001 # tijdstap (s)
t_end = 10 # eindtijd (s)
u_start = 0 # uitwijking van de massa op t=0
v_start = 0 # snelheid van de massa op t=0
W_TNT = 209
# explosion properties
t0 = 0.19
P_r = 200000

timesteps = np.arange(t_start, t_end + dt, dt)
P_R, t_0 = func_expl_par(W_TNT)
```

```
In [5]: Z_R = 1 / (W_TNT**(1/3))
# Printing the scaled distance for determining P_S0 and t_0
print(f'The scaled distance Z is {round(Z_R, 3)}')
print(t0 * (W_TNT**(1/3)) * 10**-3)
```

```
The scaled distance Z is 0.169
0.0011275497066759888
```

Getting all relevant parameters

```
In [6]: %run FunctionsBEP.ipynb

# Moment capacities, curvature end EI
M_pl_A, kappa_A, EI_A, x_uA = func_4(cover_AB, A_s_A)
M_pl_B, kappa_B, EI_B, x_uB = func_4(cover_AB, A_s_B)
M_pl_C, kappa_C, EI_C, x_uC = func_4(cover_C, A_s_C)

# Deflections
q0, w_C0 = func_w0()
q1, w_C1 = func_w1()
q2, w_C2 = func_w2()
q3, w_C3 = func_w3()

#starting conditions
y0 = np.array([v_start, 0]) # starting conditions

#stiffnesses
k1, k2, k3, k4 = func_k()
```

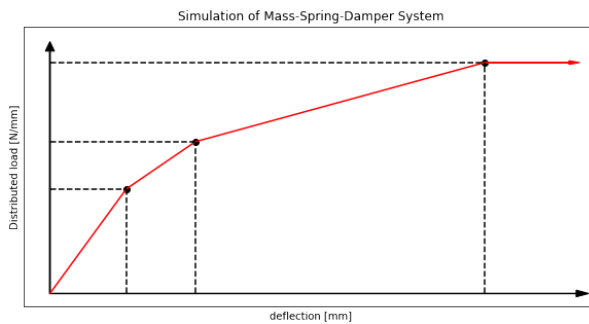
Forming of the three hinges

```
In [7]: fig, ax = plt.subplots(1, 1, figsize=(10,5))
w_curve, = ax.plot([0, w_C0, w_C1, w_C2, w_C3, 1.2*w_C3], [0, q0, q1, q2, q3, q3], 'r')
ax.arrow(0, 0, 0, int(q3*1.05), head_width = 5, width = 0.5, head_length=10, ec='k', fc='k')
ax.arrow(0, 0, int(1.21*w_C3), 0, head_width = 7, width = 0.5, head_length=7, ec='k', fc='k')
ax.arrow(int(w_C3), int(q3), int(0.2*w_C3), 0, head_width = 4, width = 0.5, ec='r', fc='r')

W = [w_C1, w_C2, w_C3]
q = [q1, q2, q3]

for i in range(3):
    ax.plot(0, W[i]), (q[i], q[i]), color='k', linestyle='--')
    ax.plot(W[i], W[i]), (0, q[i]), color='k', linestyle='--')
ax.scatter(x=[w_C1, w_C2, w_C3], y=[q1, q2, q3], c='k')
ax.plot(w_C3*1.1, q3*1.1)

ax.set_title('Simulation of Mass-Spring-Damper System')
ax.set_xlabel('deflection [mm]')
ax.set_ylabel('Distributed load [N/mm]')
ax.set_xticks([])
ax.set_yticks([])
ax.grid()
plt.show()
```



Calculating the deflection

```
In [8]: # Parallel
def func_parallel_parameters():
    L = 7200
    b = 3000
    h = 600
    m = 2650 * L * b * h * 1e-9
    k1 = k2 = 8271
    k3 = 1633
    k4 = 0
    w_C1 = w_C2 = 112.3
    w_C3 = 368.0
    return m, k1, k2, k3, k4, w_C1, w_C2, w_C3

def func_perpendicular_paramaters():
    L = 6700
    b = 3200
    h = 600
    m = 2650 * L * b * h * 1e-9
    k1 = 17187
    k2 = 8992
    k3 = 3484
    k4 = 0
    w_C1 = 40.1
    w_C2 = 80.1
    w_C3 = 239.7
    return m, k1, k2, k3, k4, w_C1, w_C2, w_C3

m, k1, k2, k3, k4, w_C1, w_C2, w_C3 = func_parallel_parameters()
m, k1, k2, k3, k4, w_C1, w_C2, w_C3 = func_perpendicular_paramaters()
c = 0
```

```
In [9]: %run FunctionsBEP.ipynb

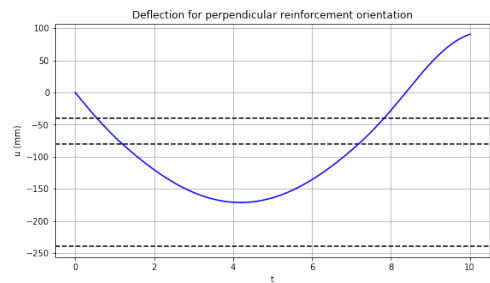
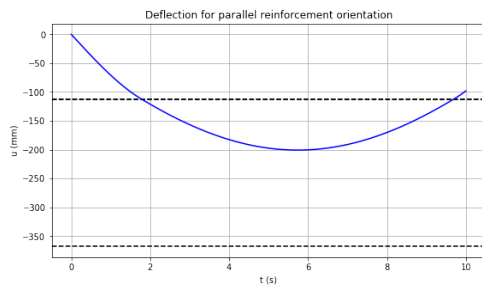
fig, [ax1, ax2] = plt.subplots(nrows=1, ncols=2, figsize=(20, 5))

m, k1, k2, k3, k4, w_C1, w_C2, w_C3 = func_parallel_parameters()
v, u, f = func_run(y0, timesteps, dt)
ax1.axhline(-w_C1, color='k', linestyle='--', label=r'$w_{1}$')
ax1.axhline(-w_C2, color='k', linestyle='--', label=r'$w_{2}$')
ax1.axhline(-w_C3, color='k', linestyle='--', label=r'$w_{3}$')
ax1.plot(timesteps[:len(u)], u, color='b', label=r'$h_{expl}$' f' = ')

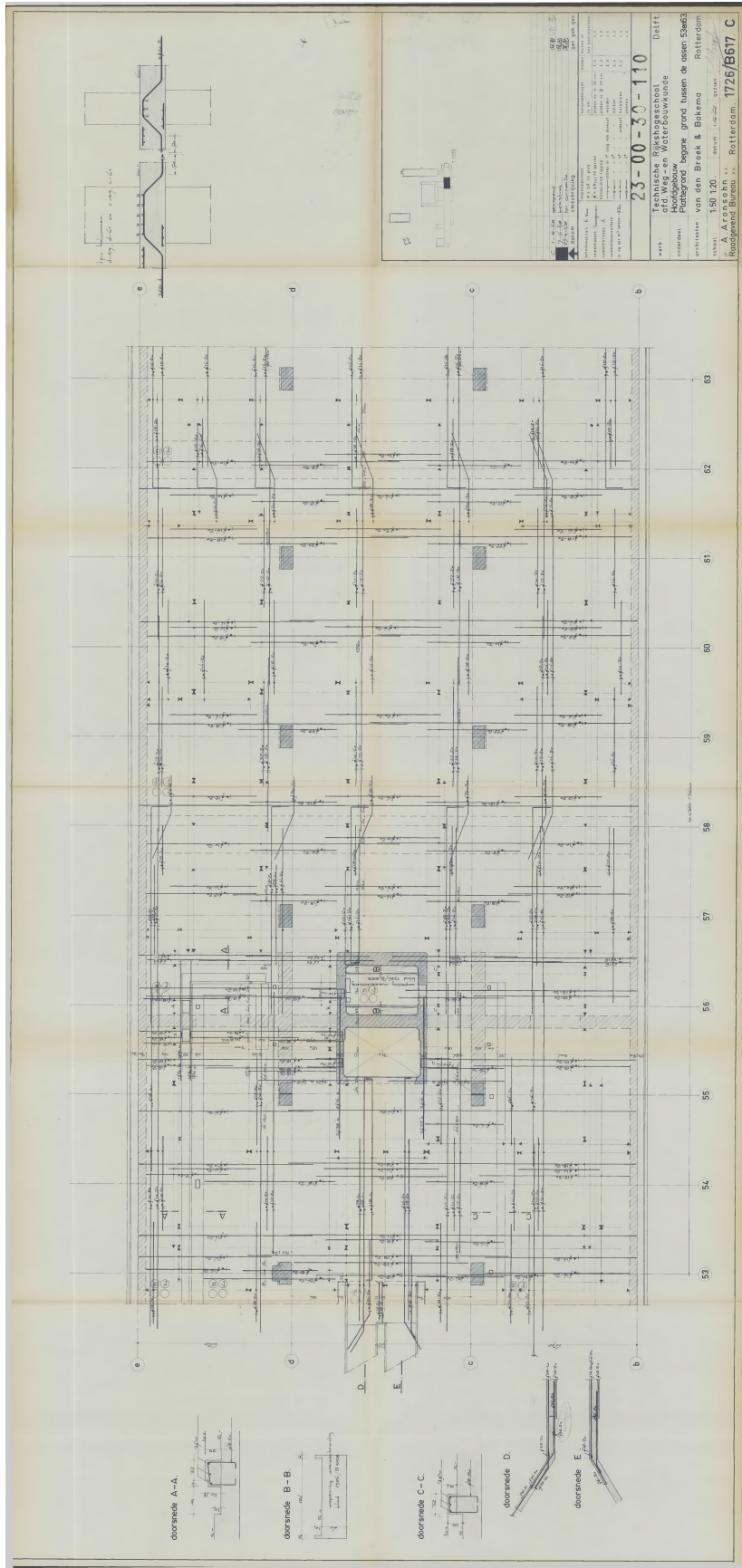
m, k1, k2, k3, k4, w_C1, w_C2, w_C3 = func_perpendicular_paramaters()
v, u, f = func_run(y0, timesteps, dt)
ax2.axhline(-w_C1, color='k', linestyle='--', label=r'$w_{1}$')
ax2.axhline(-w_C2, color='k', linestyle='--', label=r'$w_{2}$')
ax2.axhline(-w_C3, color='k', linestyle='--', label=r'$w_{3}$')
ax2.plot(timesteps[:len(u)], u, color='b', label=r'$h_{expl}$' f' = ')

ax1.set_title('Deflection for parallel reinforcement orientation')
ax1.set_xlabel('t (s)')
ax1.set_ylabel('u (mm)')
ax1.grid()

ax2.set_title('Deflection for perpendicular reinforcement orientation')
ax2.set_xlabel('t')
ax2.set_ylabel('u (mm)')
ax2.grid()
```

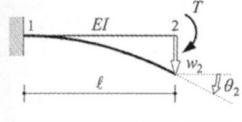
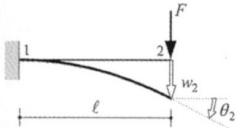
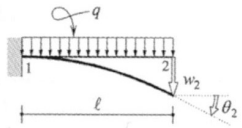
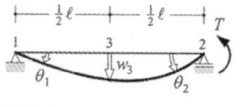
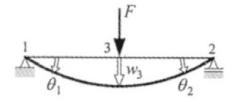
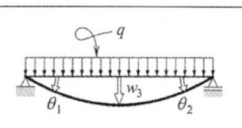
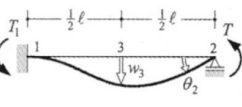
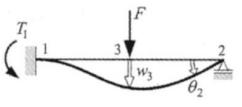
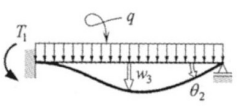
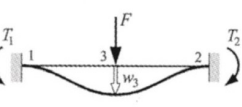
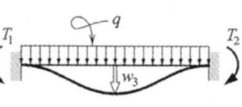


Appendix B. CEG blue print



Aronsohn, A. (Van den Broek & Bakema) (1968)

Appendix C. Forget-Me-Nots

(1)		$\theta_2 = \frac{Tl}{EI}$	$w_2 = \frac{Tl^2}{2EI}$
(2)		$\theta_2 = \frac{Fl^2}{2EI}$	$w_2 = \frac{Fl^3}{3EI}$
(3)		$\theta_2 = \frac{ql^3}{6EI}$	$w_2 = \frac{ql^4}{8EI}$
(4)		$\theta_1 = \frac{1}{6} \frac{Tl}{EI}; \theta_2 = \frac{1}{3} \frac{Tl}{EI}; w_3 = \frac{1}{16} \frac{Tl^2}{EI}$	
(5)		$\theta_1 = \theta_2 = \frac{1}{16} \frac{Fl^2}{EI}; w_3 = \frac{1}{48} \frac{Fl^3}{EI}$	
(6)		$\theta_1 = \theta_2 = \frac{1}{24} \frac{ql^3}{EI}; w_3 = \frac{5}{384} \frac{ql^4}{EI}$	
(7)		$\theta_2 = \frac{1}{4} \frac{Tl}{EI}; w_3 = \frac{1}{32} \frac{Tl^2}{EI}; T_1 = \frac{1}{2} T$	
(8)		$\theta_2 = \frac{1}{32} \frac{Fl^2}{EI}; w_3 = \frac{7}{768} \frac{Fl^3}{EI}; T_1 = \frac{3}{16} Fl$	
(9)		$\theta_2 = \frac{1}{48} \frac{ql^3}{EI}; w_3 = \frac{1}{192} \frac{ql^4}{EI}; T_1 = \frac{1}{8} ql^2$	
(10)		$w_3 = \frac{1}{192} \frac{Fl^3}{EI}; T_1 = T_2 = \frac{1}{8} Fl$	
(11)		$w_3 = \frac{1}{384} \frac{ql^4}{EI}; T_1 = T_2 = \frac{1}{12} ql^2$	

References

- Aronsohn, A. (Van den Broek & Bakema) (1968). *Technische Rijkshogeschool afd. Weg-en Waterbouwkunde: Hoofdgebouw plattegrond begane grond tussen de assen 53 en 63* [technische tekening no. 23-00-30-110]. campus real estate facility management, technisch informatie beheer.
- Baker, W., Cox, P., Westine, P., Kulesz, J., and R.A, S. (1983). *Explosion Hazards and Evaluation*. Elsevier.
- Braam, C. and Lagendijk, P. (2011). *Constructie leer Gewapend Beton*. Æneas.
- Dewey, J. (2018). *Blast Effects. Shock Wave and High Pressure Phenomena*. Springer, Cham.
- Engineers of U.S. Army Corps (2008). Structures to resist the effects of accidental explosions.
- Gebbeken, N. and Krauthammer, T. (2013). *Understanding the dynamic response of concrete to loading: practical examples*, pages 338–364, 365e–369e. Woodhead Publishing Limited.
- GICHD (2017). Explosive weapon effects – final report. Technical report, GICHD.
- GICHD (2022). Explosive ordinance guide for ukraine. Technical report, GICHD.
- Karlos V. and Solomos G. (2013). Calculation of blast loads for application to structural components - jrc technical reports. Technical report, Institute for the Protection and Security of the Citizen.
- Magnussen, J. (2007). Structural concrete elements subjected to air blast loading. RFE/RL (2024). Explainer: The 'kamikaze' drones iran used to attack israel.
- Saab, F. (2023). Basement bomb shelter feasibility in the civil engineering building, an analysis of structural integrity and safety measures. Master's thesis, Technische Universiteit Delft.
- Temsah, Y., e. a. (2017). Single degree of freedom approach of a reinforced concrete beam subjected to blast loading. *1st International Turkish World Engineering and Science Congress in Antalya*.
- Vuik, C., Vermolen, F., van Gijzen, M., and Vuik, M. (2016). *Numerical Methods for Ordinary Differential Equations*. Delft Academic Press.
- Weggel, D. (2010). *Blast threats and blast loading*, book section 1, pages 3–43. Woodhead Publishing Limited.
- Wei, W., et al. (2023). Modification of sdof model for reinforced concrete beams under close-in explosion. *Defence Technology*, 20:162–186.
- World Today News (2023). The expert revealed what drones the russian federation could attack kyiv.